Supporting Information

Stimuli responsive Zn(II) complexes showing structural conversion and on/off switching of catalytical properties

So Hyeon Kwon[a], Sunwoo Lee,[b] Jacopo Tessarolo[*,b], Haeri Lee[*,a]

[a]Department of Chemistry, Hannam University, Daejeon, 34054, Republic of Korea

[b]Department of Chemistry, Chonnam National University, Gwangju, 61186, Republic of Korea

*Corresponding authors: haeri.lee@hnu.ac.kr; jacopo@jnu.ac.kr

Contents

1. General procedures

All chemicals were obtained from commercial sources and used without further purification. NMR measurements for ligand were all conducted at 298 K on Varian USA Unity-Inova 500 at the Seoul Center of the Korea Basic Science Institute (KBSI). Mass analyses were carried out by MALDI/ESI Synapt Hight-Dimensional Mass Spectrometer at the Ochang Center of KBSI. Magritek spinsolve 60 ULTRA (^{1}H, ^{19}F) were used for catalytic reaction monitoring. Thermogravimetric analyses all except $[Zn\mathbf{L}]_n$ were carried out under a N_2 atmosphere at a scan rate 10 ℃/min using TA SDT Q600 and DSC Q200 at Busan center of KBSI. Thermogravimetric analysis for $[Zn\mathbf{L}]_n$ was measured by Thermogravimetry Analyzer of Netzsch (TG 209 F3 Tarsus) at Hannam University. All infrared spectra were obtained using IR Spirit, Shimadzu. Powder X-ray diffraction patterns were collected by D2 Phaser at Hannam University.

2. Synthesis of ligands and zinc(II) complexes

2.1 Preparation of the ligand

*2.1.1 (E)-N',N',N'',N''-tetra(2-pyridiyl)-2-butuene-1,4-diaine (**L**)*

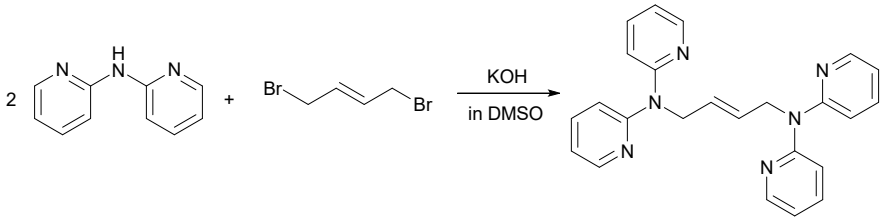

Figure S1. Synthetic procedure for **L**.

To a stirred solution of 2,2'-dipyridylamine (1.82 g, 10.5 mmol) in 1.5 mL DMSO, grinded KOH (0.71 g, 12 mmol) were added. The reaction mixture was stirred for 21 h at room temperature before the addition of *trans*-1,4-dibromo-2-butene (1.09 g, 5 mmol) in DMSO (1.5 mL). After further stirring for 3 h at r.t., the mixture was filtered. DMSO was removed by extraction with $CHCl_3$ and water. Organic layer were dried by $MgSO_4$. Then crude product was purified by column chromatography (ethyl acetate/*n*-hexane, 50%) to afford the product as a yellow crystalline solid (1.4 g, 72% yield). m.p. 117 °C. ^{1}H NMR (800 MHz, CD_3OD, 298 K, δ): 8.20 (dd, J = 5.0, 1.9 Hz, 4H), 7.60 (dd, J = 7.2, 2.0 Hz, 4H), 6.97 (d, J = 8.3 Hz, 4H), 6.95 (ddd, J = 7.2, 4.9, 0.9 Hz, 4H), 5.80 – 5.72 (m, 2H), 4.73 – 4.65 (m, 4H). ^{13}C NMR (200 MHz, CD_3OD, 298K, δ): 156.94, 147.46, 137.84, 128.44, 117.41, 115.22, 49.37. IR (KBr, cm^{-1}): 1582s, 1559m, 1467s, 1423s, 1381m, 1361m, 1324m, 1282w, 1256w, 1238s, 1166w, 1152w, 1092w, 997w, 865w, 778m, 643w, 611w. HR-ESI-Mass (m/z): 395.1983 (calcd $[C_{24}H_{22}N_6 + H^+]^+$ = 395.1979).

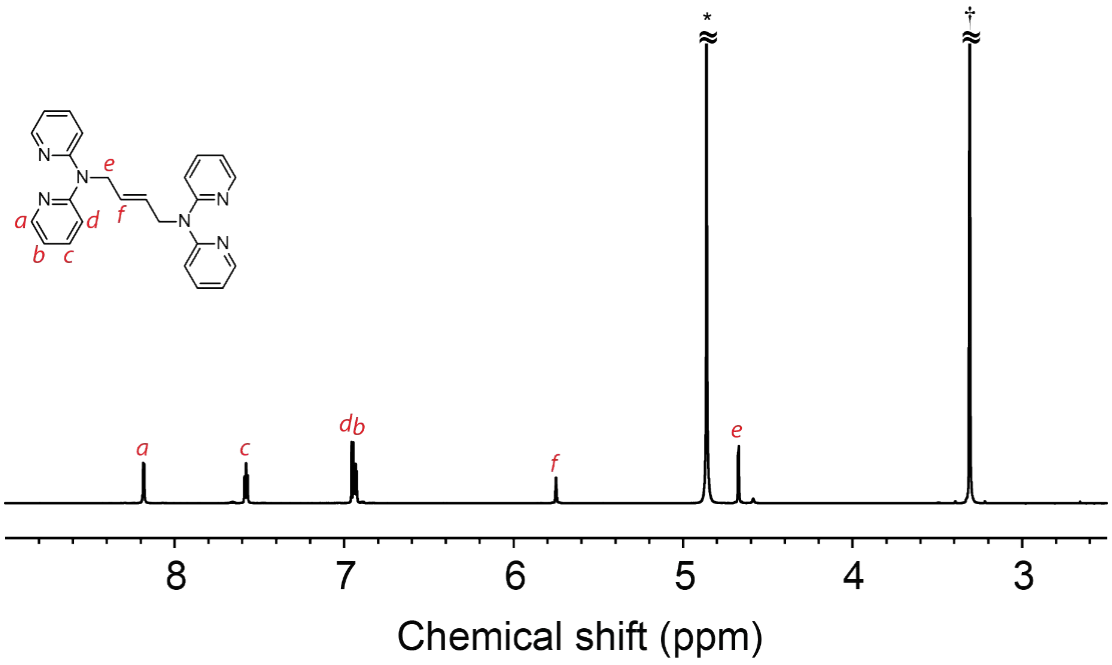

Figure S2. ^{1}H NMR spectrum for **L** in CD_3OD (†Solvent residual signal, *HDO).

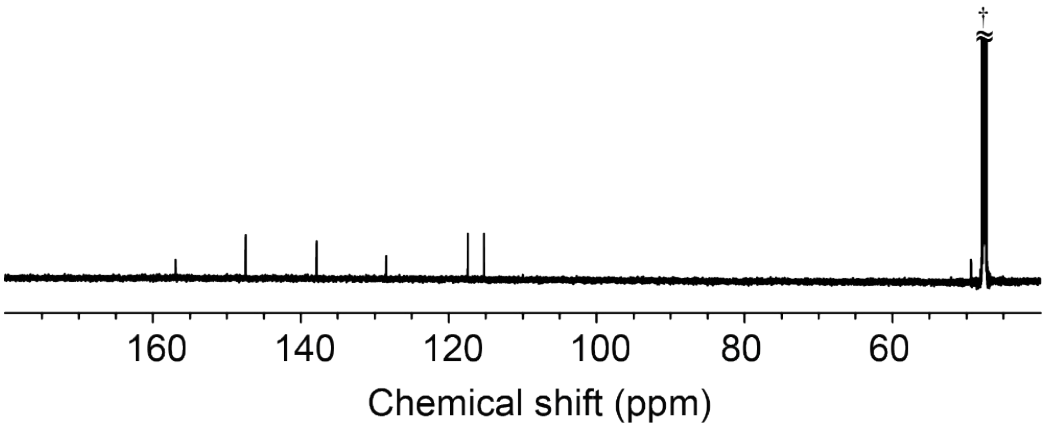

Figure S3. ^{13}C NMR spectrum for **L** in CD_3OD (†solvent).

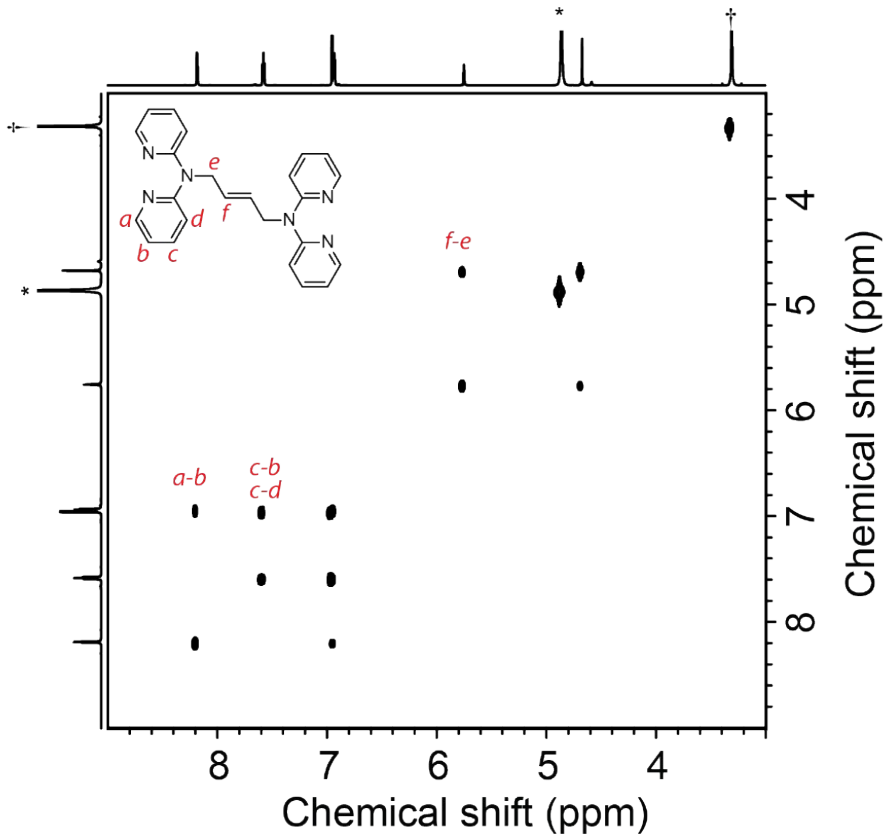

Figure S4. ^{1}H-^{1}H COSY spectrum for **L** in CD_3OD (†Solvent residual signal, *HDO).

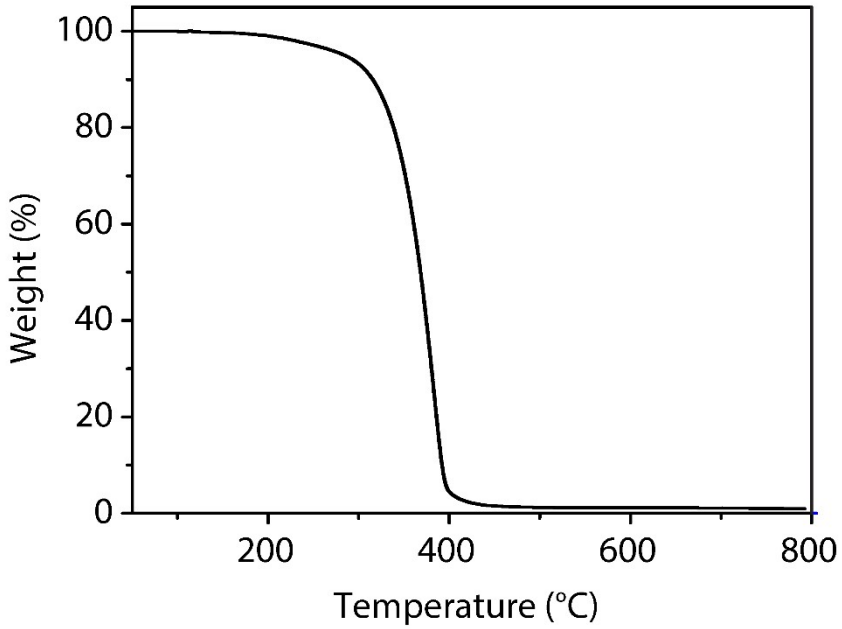

Figure S5. TG analysis for **L** (dec. 117 °C, remains: 0% at 800 °C).

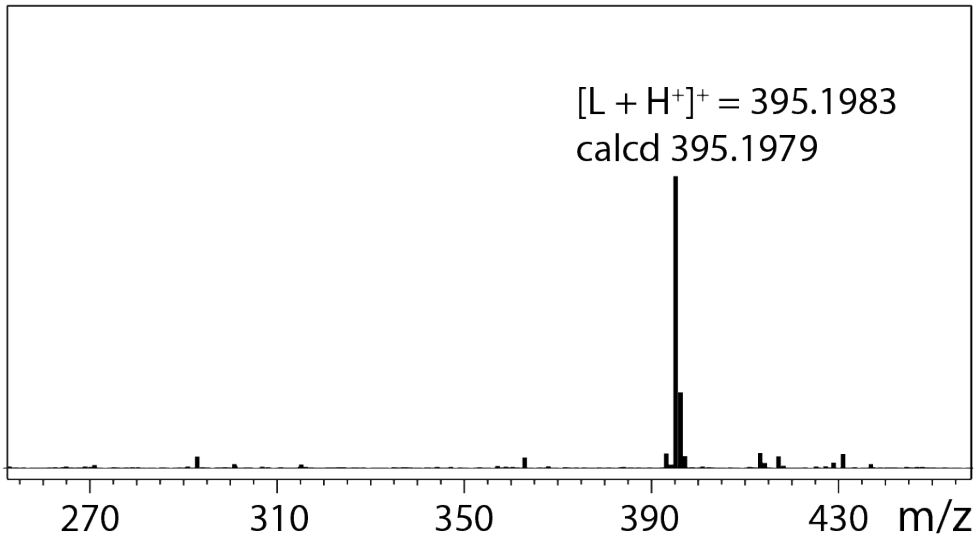

Figure S6. High-resolution ESI-Mass spectrum for **L**, m/z 395.1983 (calcd $[C_{24}H_{22}N_6+H^+]^+$ = 395.1979).

2.2 Synthesis of zinc(II) complexes

*2.2.1 Synthesis of [Zn_2Cl_4**L**]*

A mixed solution of methanol and dichloromethane (10 mL) of (*E*)-*N',N',N'',N''*-tetra(2-pyridyl)-2-butene-1,2-diamine (**L**) (39 mg, 0.1 mmol) was slowly added to a methanol solution (10 mL) of zinc(II) chloride (14 mg, 50 μmol). After a day, colorless crystals of Zn_2Cl_4**L** were obtained in 89% (30 mg) yield. m.p. 316 °C (dec.). IR (KBr pellet, cm^{-1}): 3068w, 3031w, 2876w, 1602s, 1574s, 1489m, 1459s, 1437s, 1379m, 1347s, 1317w, 1296w, 1274w, 1243s, 1209w, 1160m, 1137m, 1083w, 1047m, 1026m, 998w, 983w, 885m, 797s, 774s, 756s, 651w, 603m, 485w, 423m.

*2.2.2 Synthesis of [Zn_2Br_4**L**]*

[Zn_2Br_4**L**] was prepared in the same manner as [Zn_2Cl_4**L**], using $ZnBr_2$ instead of $ZnCl_2$ in a 80% (34 mg) yield. m.p. 320 °C (dec.). IR (KBr pellet, cm^{-1}): 1600s, 1574s, 1488m, 1467s, 1457s, 1445s, 1376w, 1348m, 1242m, 1209w, 1161w, 1137w, 1047m, 1026m, 995w, 980w, 884m, 797s, 774s, 754s, 652w, 423m.

*2.2.3 Synthesis of [Zn_2I_4**L**]*

[Zn_2I_4**L**] was prepared in the same manner as [Zn_2Cl_4**L**], using ZnI_2 instead of $ZnCl_2$ in a 78% (40 mg) yield. m.p. 320 °C (dec.) IR (KBr pellet, cm^{-1}): 3063w, 3024w, 2869w, 1602s, 1572s, 1489m, 1471s, 1456s, 1438s, 1379m, 1336s, 1302w, 1234s, 1162m, 1137m, 1080w, 1062w, 1042w, 1026m, 990w, 970w, 887m, 777s, 747m, 645w, 608w, 580w, 414w.

*2.2.4 Synthesis of cis- and trans-[Zn**L**$(MeOH)_2]_n(ClO_4)_{2n}$·2MeOH (cis-, trans-[Zn**L**$]_n$)*

A methanol solution of **L** (47 mg, 0.12 mmol) was added into a methanol solution of $Zn(ClO_4)_2·6H_2O$ (45 mg, 0.12 mmol). After 2 days, colorless crystals of $[Zn\mathbf{L}(MeOH)_2]_n(ClO_4)_{2n}·2n$MeOH were obtained in 84% (94 mg) yield. m.p. 318 °C (dec.). IR (KBr pellet, cm^{-1}): 3063w, 3012w, 2930w, 2875w, 1637m, 1601s, 1582s, 1559m, 1468s, 1445s, 1425s, 1377m, 1347m, 1324m, 1298m, 1274m, 1240m, 1208m, 1142s (ν ClO_4^-), 1115s, 1085s, 1026m, 979m, 940w, 884m, 797m, 774m, 755m, 636s, 625s, 603w, 484w, 422w.

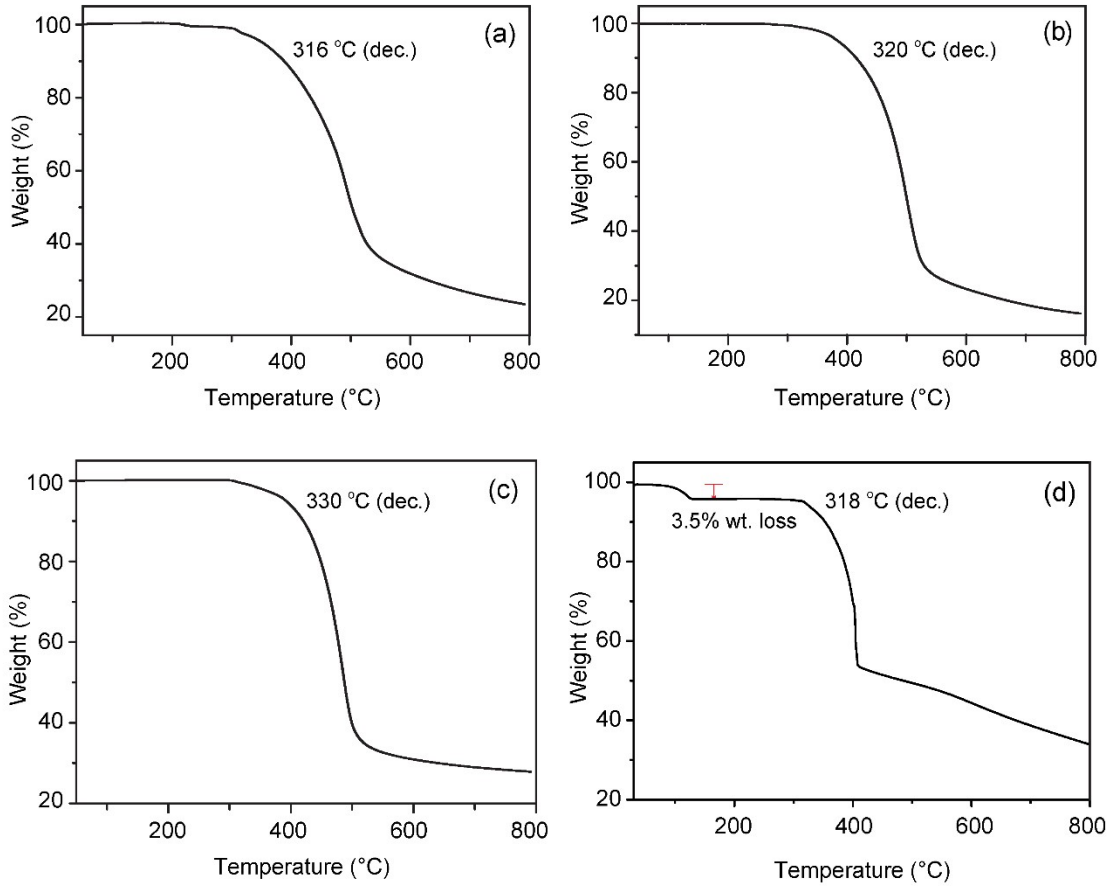

Figure S7. TG analyses for $[Zn_2Cl_4\mathbf{L}]$ (a), $[Zn_2Br_4\mathbf{L}]$ (b), $[Zn_2I_4\mathbf{L}]$ (c), and $[Zn\mathbf{L}]_n$ (d) under N_2 atmosphere, scan rate = 10 °C/min.

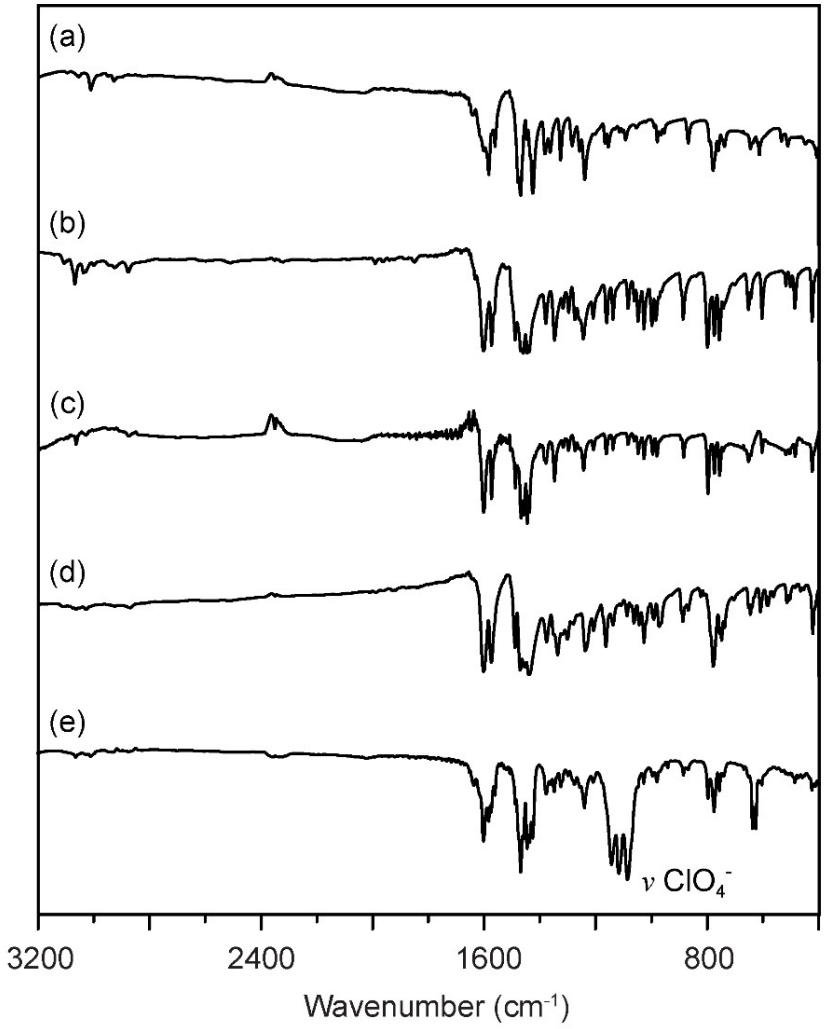

Figure S8. FT-IR spectra (in KBr mode) for **L** (a), $[Zn_2Cl_4\mathbf{L}]$ (b), $[Zn_2Br_4\mathbf{L}]$ (c), and $[Zn_2I_4\mathbf{L}]$ (d), and $[Zn\mathbf{L}]_n$ (e).

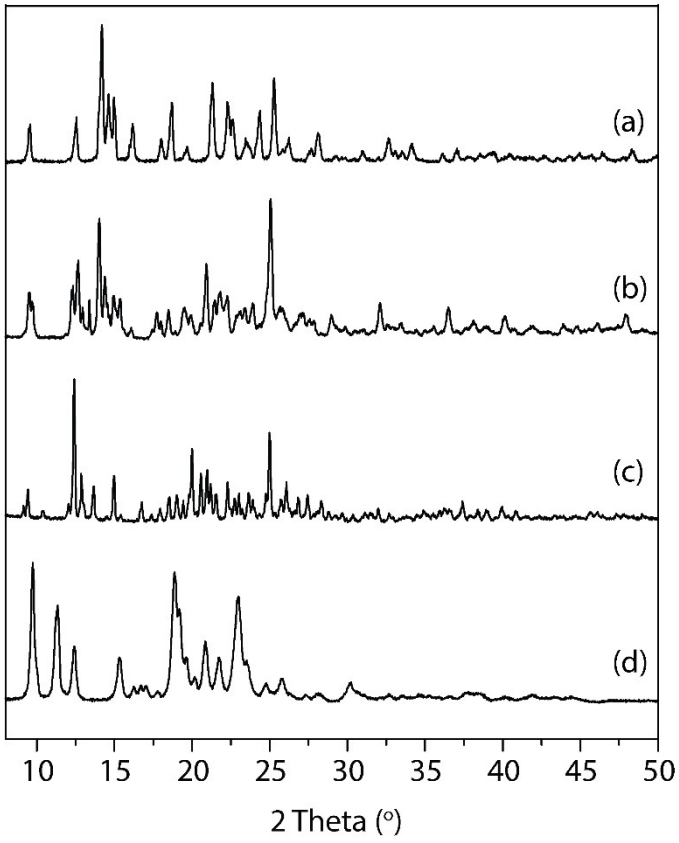

Figure S9. Powder XRD patterns for [Zn_2Cl_4**L**] (a), [Zn_2Br_4**L**] (b), and [Zn_2I_4**L**] (c), and [Zn**L**]$_n$ (d).

3. X-ray crystallography

3.1 Data collection details

X-ray diffraction data for were collected on a Bruker APEX III for [Zn_2X_4**L**] (X = Cl, Br, I), Bruker D8 Venture for [Zn**L**]$_n$ coated with Paraton-*N* oil. Data were collected in-house X-ray diffractometer equipped with an INCOATEC microfocus sealed tube (IμS 3.0) using Mo K_α. For all X-ray diffraction data, thirty-six (36) frames of 2D diffraction images from CCD detector were collected and processed to obtain the cell parameters and orientation matrix. The data were corrected for Lorentz and polarization effects. All structures were solved by intrinsic phasing/direct methods using SHELXT[1] and refined with SHELXL (2018/3)[2] for full-matrix least-squares routines on F[2] and ShelXle[3] as a graphical user interface. The non-hydrogen atoms were refined anisotropically, and the hydrogen atoms were placed in calculated positions and refined only for the isotropic thermal factors. The crystal parameters and procedural information corresponding to the data collection and structure refinement are listed in Table S1.

Table S1. Crystal data for **L**, $[Zn_2Cl_4\mathbf{L}]$, $[Zn_2Br_4\mathbf{L}]$, $[Zn_2I_4\mathbf{L}]$, *trans*-$[Zn\mathbf{L}]_n$·2MeOH, and *cis*-$[Zn\mathbf{L}]_n$·2MeOH

	L	$[Zn_2Cl_4\mathbf{L}]$	$[Zn_2Br_4\mathbf{L}]$	$[Zn_2I_4\mathbf{L}]$
CCDC No.	2144545	2144546	2144547	2144548
Empirical formula	$C_{24}H_{22}N_6$	$C_{24}H_{22}Cl_4N_6Zn_2$	$C_{24}H_{22}Br_4N_6Zn_2$	$C_{24}H_{22}I_4N_6Zn_2$
Formula weight	394.47	667.01	844.85	1032.81
Temperature (K)	194(2)	173(2)	173(2)	193(2)
Wavelength (Å)	0.71073	0.71073	0.71073	0.71073
Crystal system	Monoclinic	Monoclinic	Monoclinic	Monoclinic
Space group	$P2_1/c$	$P2_1/n$	$P2_1/n$	$P2_1/c$
a (Å)	8.21360(10)	7.9002(8)	8.1556(4)	14.9058(3)
b (Å)	12.8837(2)	11.6313(12)	11.6931(7)	10.4325(2)
c (Å)	9.3506(2)	14.4637(14)	14.6784(8)	20.5991(4)
β (°)	97.3250(10)	90.130(3)	90.389(2)	109.4780(10)
Volume (Å^3)	981.42(3)	1329.1(2)	1399.76(13)	3019.93(10)
Z	2	2	2	4
Density (calculated) (Mg/m^3)	1.335	1.667	2.005	2.272
Absorption coefficient (mm^{-1})	0.083	2.233	7.448	5.702
F(000)	416	672	816	1920
Crystal size (mm^3)	0.480 x 0.270 x 0.260	0.056 x 0.041 x 0.019	0.113 x 0.035 x 0.032	0.420 x 0.410 x 0.240
Theta range for data collection (°)	2.500 to 28.403	2.578 to 26.497	2.775 to 27.146	1.449 to 28.280
Index ranges	-10<=h<=10 -17<=k<=17 -12<=l<=10	-9<=h<=9 -14<=k<=14 -18<=l<=18	-10<=h<=10 -15<=k<=15 -18<=l<=18	-19<=h<=19 -13<=k<=13 -27<=l<=26
Reflections collected	16732	18583	25720	52213
Independent reflections	2450 [R(int) = 0.0230]	2738 [R(int) = 0.0909]	3073 [R(int) = 0.0878]	7464 [R(int) = 0.0307]
Completeness to theta (%)(25.242°)	99.4	99.3	99.1	99.7
Absorption correction	Semi-empirical from equivalents	Semi-empirical from equivalents	Semi-empirical from equivalents	Semi-empirical from equivalents
Max. and min. transmission	1.000 and 0.789	0.7456 and 0.6543	0.7455 and 0.4086	1.000 and 0.789
Refinement method	Full-matrix least-squares on F^2	Full-matrix least-squares on F^2	Full-matrix least-squares on F^2	Full-matrix least-squares on F^2
Data / restraints / parameters	2450 / 0 / 136	2738 / 0 / 164	3073 / 0 / 164	7464 / 0 / 325
Goodness-of-fit on F^2	1.044	1.161	1.131	1.031
Final R indices [I>2sigma(I)]	R1 = 0.0405 wR2 = 0.1073	R1 = 0.0747 wR2 = 0.1247	R1 = 0.0338 wR2 = 0.0682	R1 = 0.0340 wR2 = 0.0705
R indices (all data)	R1 = 0.0444 wR2 = 0.1116	R1 = 0.0892 wR2 = 0.1295	R1 = 0.0509 wR2 = 0.0787	R1 = 0.0419 wR2 = 0.0739
Largest diff. peak and hole (e·Å^{-3})	0.255 and -0.239	0.507 and -0.909	0.487 and -0.709	1.724 and -1.502

Table S1. *(Continued)*

	trans-[Zn**L**]$_n$·2MeOH	*cis*-[Zn**L**]$_n$·MeOH
CCDC No.	2331257	2364848
Empirical formula	$C_{28}H_{38}Cl_2N_6O_{12}Zn$	$C_{54}H_{68}Cl_4N_{12}O_{22}Zn_2$
Formula weight	786.91	1509.74
Temperature (K)	173(2)	173(2)
Wavelength (Å)	0.71073	0.71073
Crystal system	Monoclinic	Triclinic
Space group	$P2_1/n$	P-1
a (Å)	7.9366(6)	10.9854(9)
b (Å)	19.2414(16)	12.5818(11)
c (Å)	11.2733(9)	25.124(2)
α (°)	-	81.710(2)
β (°)	96.936(2)	80.594(3)
γ (°)	-	75.975(2)
Volume (Å^3)	1709.0(2)	3303.8(5)
Z	2	2
Density (calculated) (Mg/m^3)	1.529	1.518
Absorption coefficient (mm^{-1})	0.944	0.971
F(000)	816	1560
Crystal size (mm^3)	0.150 x 0.080 x 0.080	0.081 x 0.049 x 0.037
Theta range for data collection (°)	2.792 to 26.368	2.480 to 27.064
Index ranges	-9<=h<=9 -24<=k<=24 -14<=l<=14	–14<=h<=14 –16<=k<=16 –32<=l<=32
Reflections collected	61409	112356
Independent reflections	3457 [R(int) = 0.0821]	14416 [R(int) = 0.0948]
Completeness to theta (%)(25.242°)	99.2	99.90
Absorption correction	Semi-empirical from equivalents	Semi-empirical from equivalents
Max. and min. transmission	0.7454 and 0.4885	0.7455 and 0.6586
Refinement method	Full-matrix least-squares on F^2	Full-matrix least-squares on F^2
Data / restraints / parameters	3457 / 0 / 225	14416 / 723 / 1030
Goodness-of-fit on F^2	1.054	1.074
Final R indices [I>2sigma(I)]	R1 = 0.0360 wR2 = 0.0924	R1 = 0.0570 wR2 = 0.1160
R indices (all data)	R1 = 0.0421 wR2 = 0.0981	R1 = 0.0933 wR2 = 0.1334
Largest diff. peak and hole (e·Å^{-3})	0.572 and -0.489	0.685 and –0.453

Table S2. Selected bonds (Å) and angles (°) for $[Zn_2Cl_4\mathbf{L}]$, $[Zn_2Br_4\mathbf{L}]$, $[Zn_2I_4\mathbf{L}]$, *trans*-$[Zn\mathbf{L}]_n \cdot 2MeOH$, and *cis*-$[Zn\mathbf{L}]_n \cdot 2MeOH$

$[Zn_2Cl_4\mathbf{L}]$		$[Zn_2Br_4\mathbf{L}]$		$[Zn_2I_4\mathbf{L}]$	
Zn(1)-N(1)	2.045(5)	Zn(1)-N(1)	2.043(4)	Zn(1)-I(1)	2.5574(6)
Zn(1)-N(3)	2.047(5)	Zn(1)-N(3)	2.044(4)	Zn(1)-N(1)	2.037(4)
Zn(1)-Cl(2)	2.1988(19)	Zn(1)-Br(2)	2.3378(7)	Zn(1)-N(3)	2.025(3)
Zn(1)-Cl(1)	2.2173(18)	Zn(1)-Br(1)	2.3553(7)	Zn(1)-I(2)	2.5328(6)
				Zn(2)-N(4)	2.028(3)
				Zn(2)-N(6)	2.036(3)
				Zn(2)-I(3)	2.5470(6)
				Zn(2)-I(4)	2.5487(6)
N(1)-Zn(1)-N(3)	89.58(19)	N(1)-Zn(1)-N(3)	89.88(14)	N(3)-Zn(1)-N(1)	89.91(15)
N(1)-Zn(1)-Cl(2)	107.11(15)	N(1)-Zn(1)-Br(2)	108.08(10)	N(3)-Zn(1)-I(2)	114.63(10)
N(3)-Zn(1)-Cl(2)	116.00(15)	N(3)-Zn(1)-Br(2)	116.15(10)	N(1)-Zn(1)-I(2)	111.05(11)
N(1)-Zn(1)-Cl(1)	113.71(15)	N(1)-Zn(1)-Br(1)	113.45(10)	N(3)-Zn(1)-I(1)	108.86(10)
N(3)-Zn(1)-Cl(1)	107.90(14)	N(3)-Zn(1)-Br(1)	107.57(10)	N(1)-Zn(1)-I(1)	108.81(10)
Cl(2)-Zn(1)-Cl(1)	118.89(8)	Br(2)-Zn(1)-Br(1)	118.31(3)	I(2)-Zn(1)-I(1)	119.55(2)
				N(4)-Zn(2)-N(6)	88.75(13)
				N(4)-Zn(2)-I(3)	111.11(10)
				N(6)-Zn(2)-I(3)	108.87(11)
				N(4)-Zn(2)-I(4)	108.74(10)
				N(6)-Zn(2)-I(4)	117.86(10)
				I(3)-Zn(2)-I(4)	117.75(2)

Table S2. *(Continued)*

trans-[Zn**L**]$_n$·2MeOH		*cis*-[Zn**L**]$_n$·MeOH	
Zn(1)-N(1)	2.1145(17)	Zn(1)-N(48)	2.101(3)
Zn(1)-N(2)	2.1206(18)	Zn(1)-O(91)	2.120(3)
Zn(1)-O(1)	2.2026(15)	Zn(1)-N(18)	2.123(3)
		Zn(1)-N(11)	2.151(3)
		Zn(1)-N(41)	2.173(3)
		Zn(1)-O(93)	2.189(3)
		Zn(2)-N(35)	2.097(3)
		Zn(2)-N(28)	2.106(3)
		Zn(2)-N(65)$^{\#2}$	2.119(3)
		Zn(2)-N(58)$^{\#2}$	2.137(3)
N(1)-Zn(1)-N(1)$^{\#1}$	180.00(8)	N(48)-Zn(1)-O(91)	92.38(12)
N(1)-Zn(1)-N(2)$^{\#1}$	96.05(7)	N(48)-Zn(1)-N(18)	99.41(11)
N(1)$^{\#1}$-Zn(1)-N(2)$^{\#1}$	83.95(7)	O(91)-Zn(1)-N(18)	168.08(12)
N(1)-Zn(1)-N(2)	83.95(7)	N(48)-Zn(1)-N(11)	94.05(11)
N(1)$^{\#1}$-Zn(1)-N(2)	96.05(7)	O(91)-Zn(1)-O(93)	82.41(12)
N(2)$^{\#1}$-Zn(1)-N(2)	180.00(7)	N(18)-Zn(1)-N(41)	96.09(11)
N(1)-Zn(1)-O(1)$^{\#1}$	88.60(6)	N(11)-Zn(1)-N(41)	178.60(11)
N(1)$^{\#1}$-Zn(1)-O(1)$^{\#1}$	91.40(6)	N(48)-Zn(1)-O(93)	174.79(12)
N(2)$^{\#1}$-Zn(1)-O(1)$^{\#1}$	90.93(6)	O(91)-Zn(1)-O(93)	82.41(12)
N(2)-Zn(1)-O(1)$^{\#1}$	89.07(6)	N(35)-Zn(2)-O(95)	92.55(13)
N(1)-Zn(1)-O(1)	91.40(6)	N(28)-Zn(2)-O(95)	88.25(12)
N(1)$^{\#1}$-Zn(1)-O(1)	88.60(6)	N(35)-Zn(2)-O(97)	173.03(12)
N(2)$^{\#1}$-Zn(1)-O(1)	89.07(6)	N(28)-Zn(2)-O(97)	93.63(11)
N(2)-Zn(1)-O(1)	90.93(6)	O(95)-Zn(2)-O(97)	80.84(12)
O(1)$^{\#1}$-Zn(1)-O(1)	180		

$^{\#1}$-x+1,-y+1,-z+1 $^{\#2}$ x-1,y,z

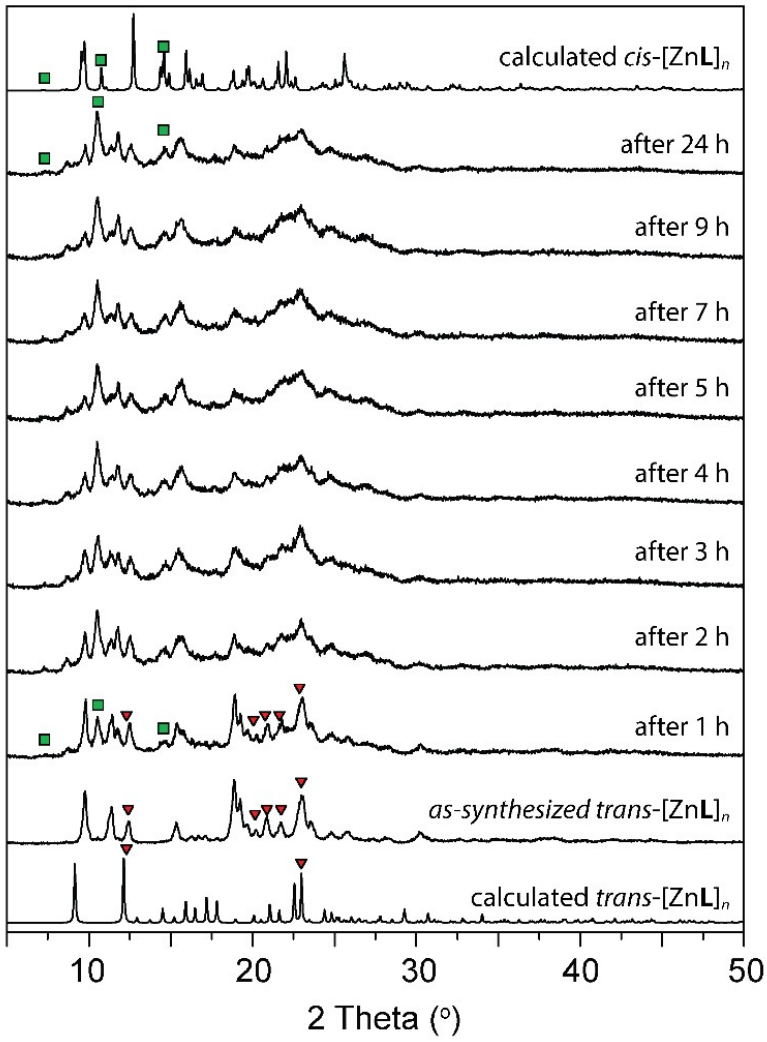

Figure S10. Powder XRD patterns for time-dependent [Zn**L**]$_n$ after exposure to methanol at 50 °C with vigorous stirring (symbol code: green, matching peaks to calculated X-ray diffraction pattern of *cis*-[Zn**L**]$_n$; red, calculated *trans*-[Zn**L**]$_n$)

4. Catalytic properties

4.1 General procedure for catalysis

Transesterification reaction of each substrate was performed in a 2 mL vials equipped with temperature controlling system with a reaction block. Phenyl acetate (**Sub-1**), p-tolyl acetate (**Sub-2**), 4-fluorophenyl acetate (**Sub-3**), pentafluorophenyl acetate (**Sub-4**), and 4-nitrophenyl acetate (**Sub-5**) were used for substrates. The temperature controller ensured a constant temperature of the reaction block with a precision of 1 K. 500 μmol of substrate in 500 μL methanol was added into the reaction vial charged with suggested amount of each Zn(II) complex. The reaction solution was vigorously stirred at 50 ℃. The reaction was monitored by Time dependent ^{1}H and ^{19}F NMR spectroscopy. Reaction mixture samples of 20 μL were obtained and diluted with 500 μL of acetone-d_6. The catalytic yields were determined by the integrating the NMR spectra corresponding to the products of both methyl acetate ($-CH_3$ or $-OCH_3$) and aryl alcohol.

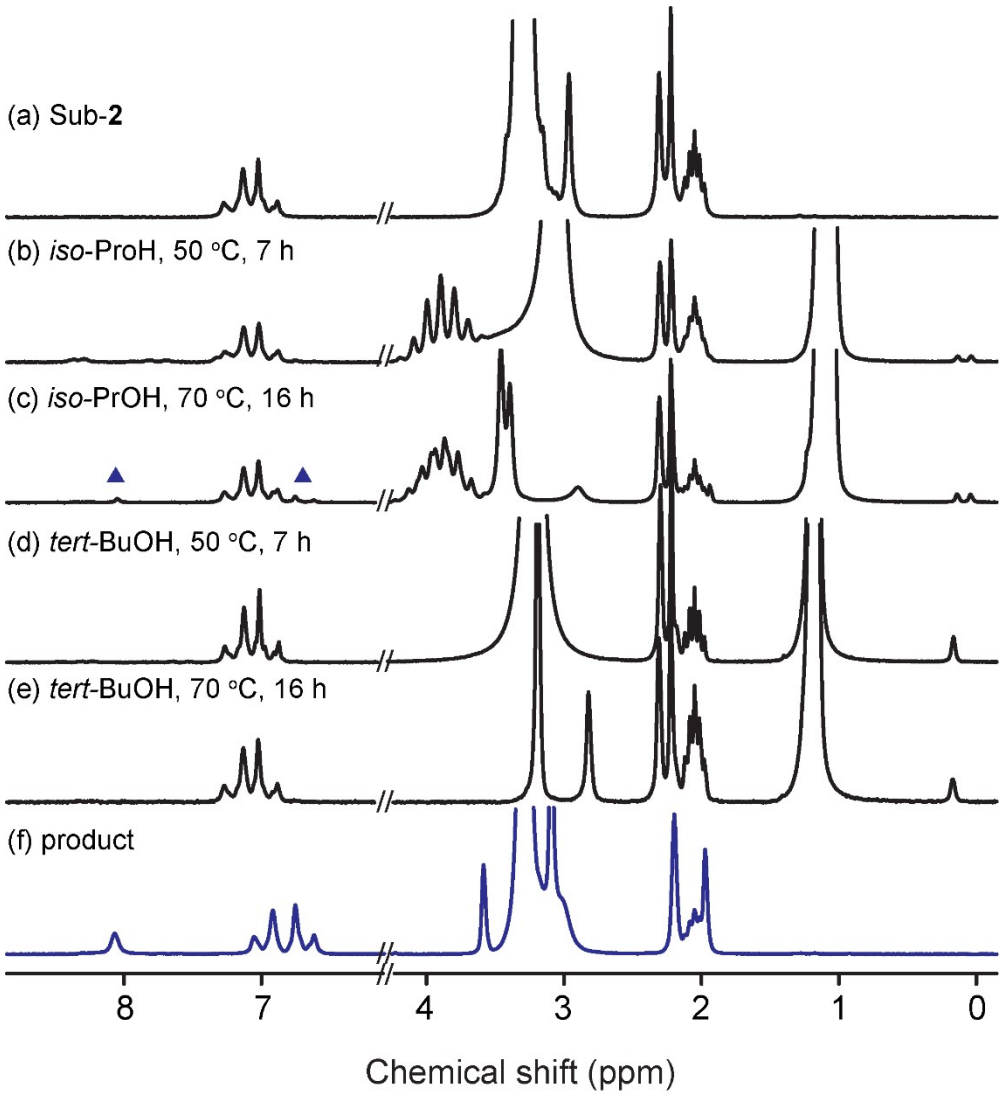

Figure S11. NMR monitoring for transesterification reaction of *p*-tolyl acetate (**Sub-2**, a) by changing alcohols. *Iso*-propanol was used for the catalytic reaction with cat. 10 mol% [Zn**L**]$_n$ under two different conditions, 50 ℃ for 7 hours and 70 ℃ for 16 hours (b, c, respectively). *Tert*-butanol was used for the catalytic reaction with cat. 10 mol% [Zn**L**]$_n$ at 50 ℃ for 7 hours and 70 ℃ for 16 hours (d, e, respectively). Blue triangles and spectrum (f) indicate the expected product.

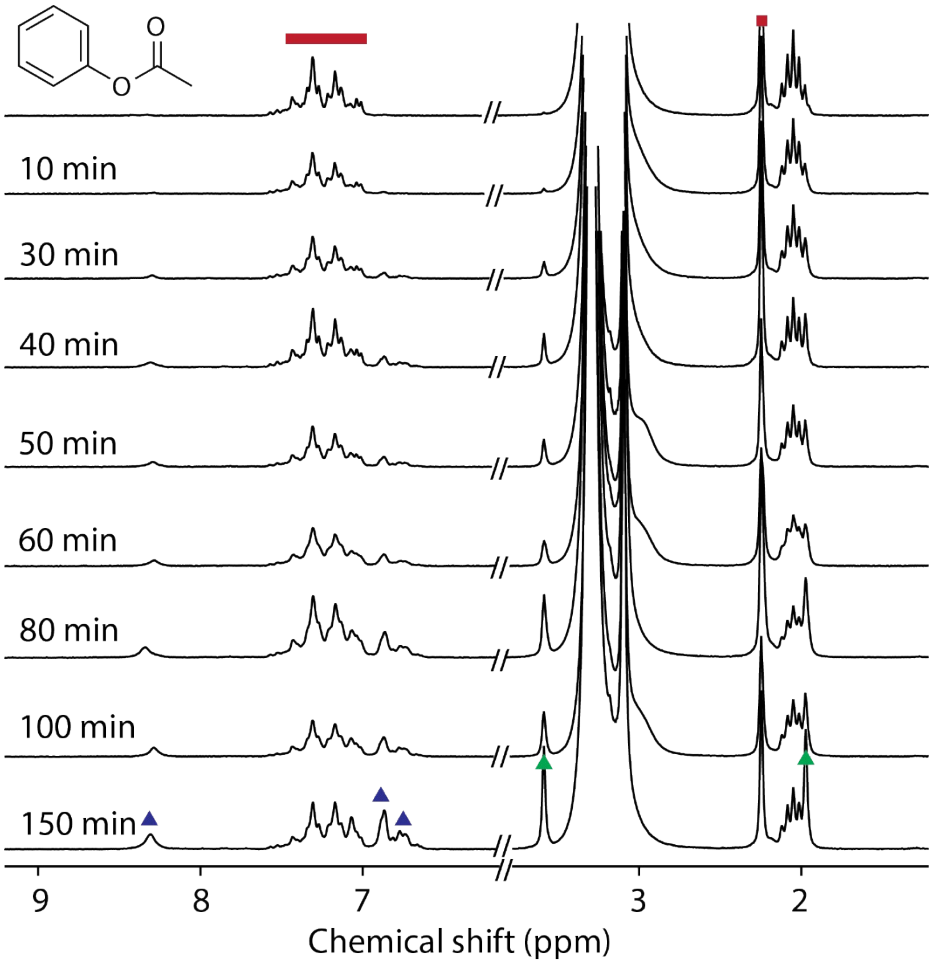

Figure S12. Time-dependent NMR monitoring for transesterification reaction of phenyl acetate (**Sub-1**, 500 μmol, 68 mg) and methanol with cat. 10 mol% (19.5 mg) $[ZnL]_n$ (red: substate, green: methyl acetate, blue: phenol).

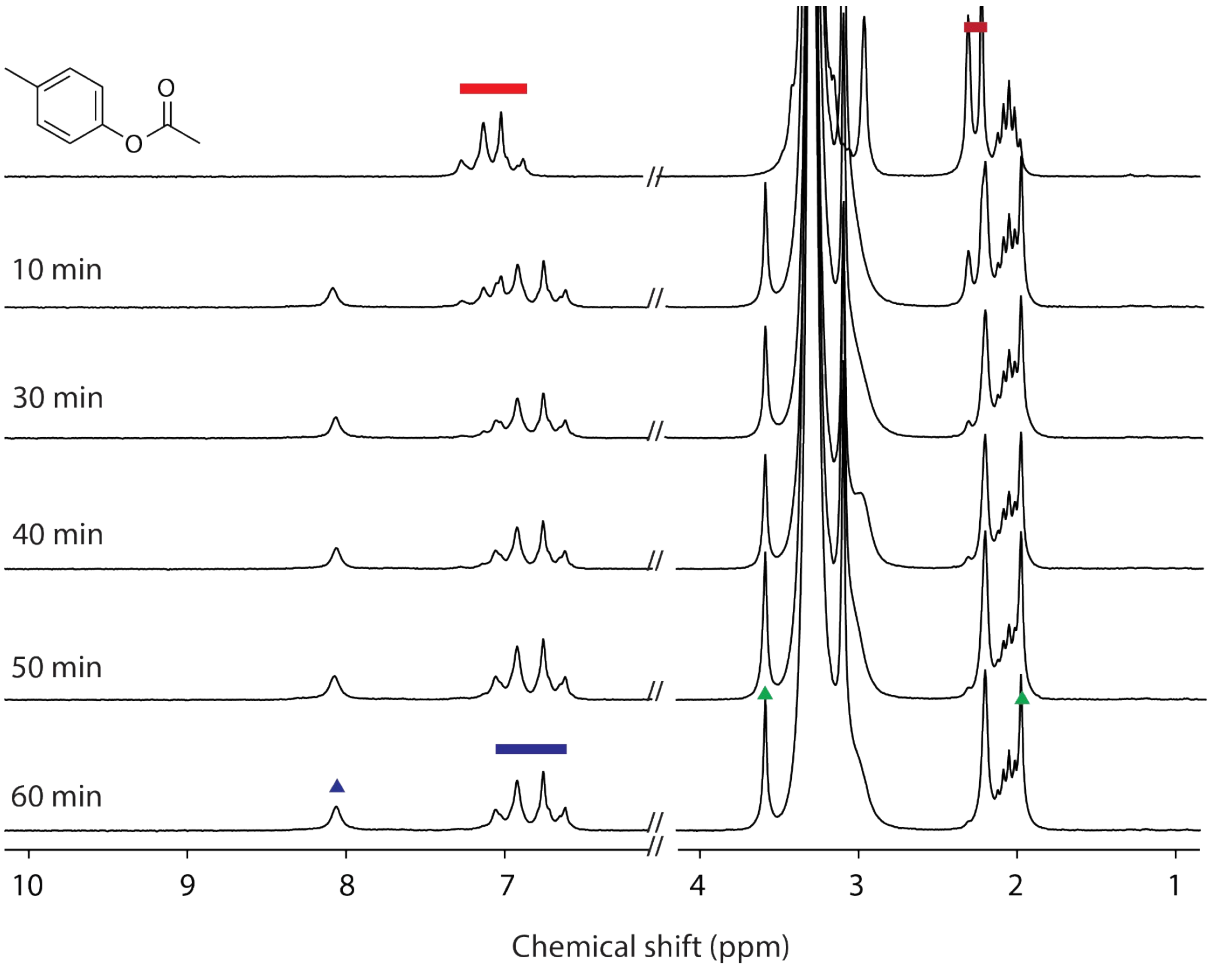

Figure S13. Time-dependent NMR monitoring for transesterification reaction of *p*-tolyl acetate (**Sub-2**, 500 μmol, 75 mg) and methanol with cat. 10 mol% (19.5 mg) $[ZnL]_n$ (red: substate, green: methyl acetate, blue: *p*-cresol).

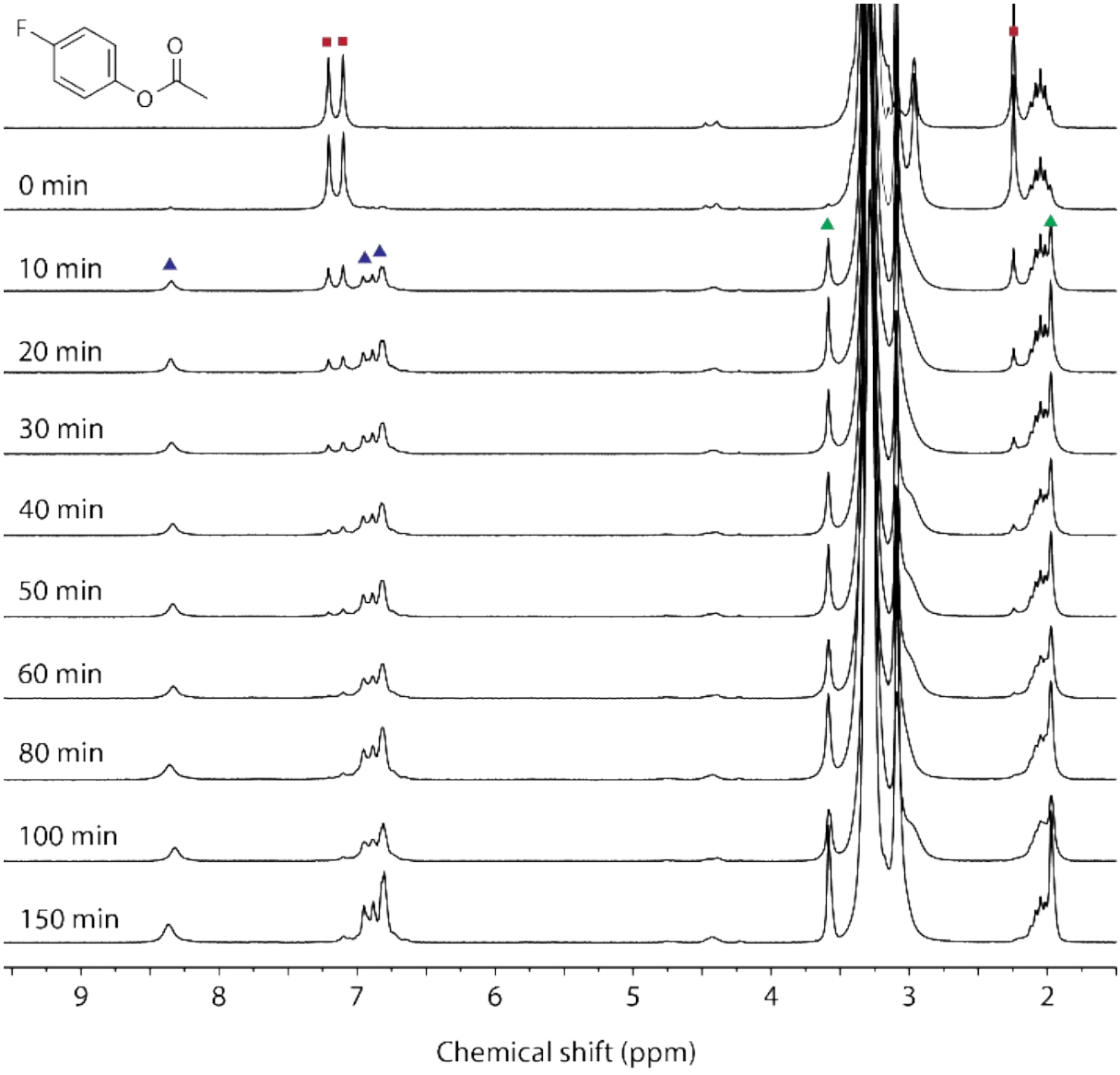

Figure S14. Time-dependent NMR monitoring for transesterification reaction of 4-fluorophenyl acetate (**Sub-3**, 500 μmol, 77 mg) and methanol with cat. 10 mol% (19.5 mg) [Zn**L**]$_n$ (red: substate, green: methyl acetate, blue: 4-fluorophenol).

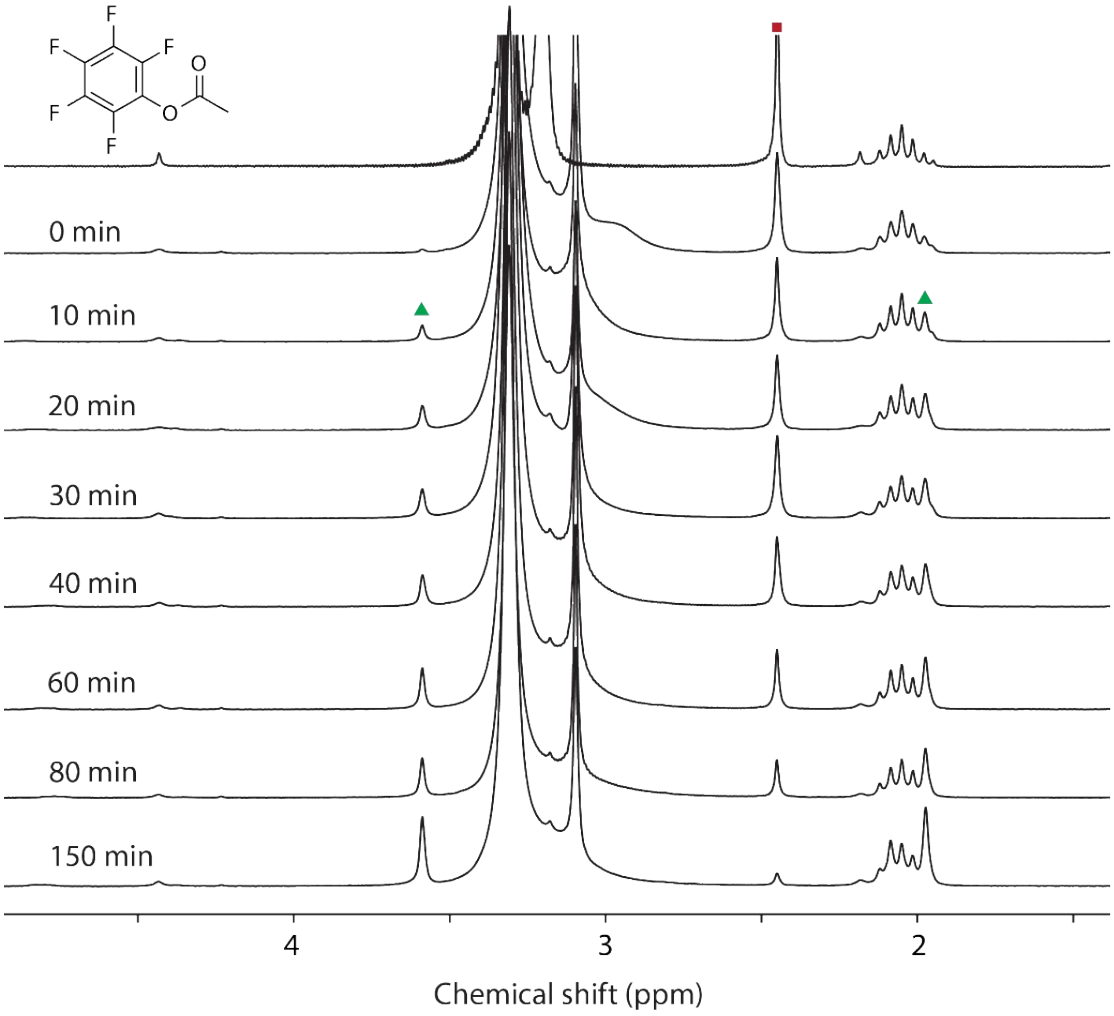

Figure S15. Time-dependent NMR monitoring for transesterification reaction of pentafluorophenyl acetate (**Sub-4**, 500 μmol, 133 mg) and methanol with cat. 10 mol% (19.5 mg) [Zn**L**]$_n$ (red: substate, green: methyl acetate, blue: pentafluorophenol).

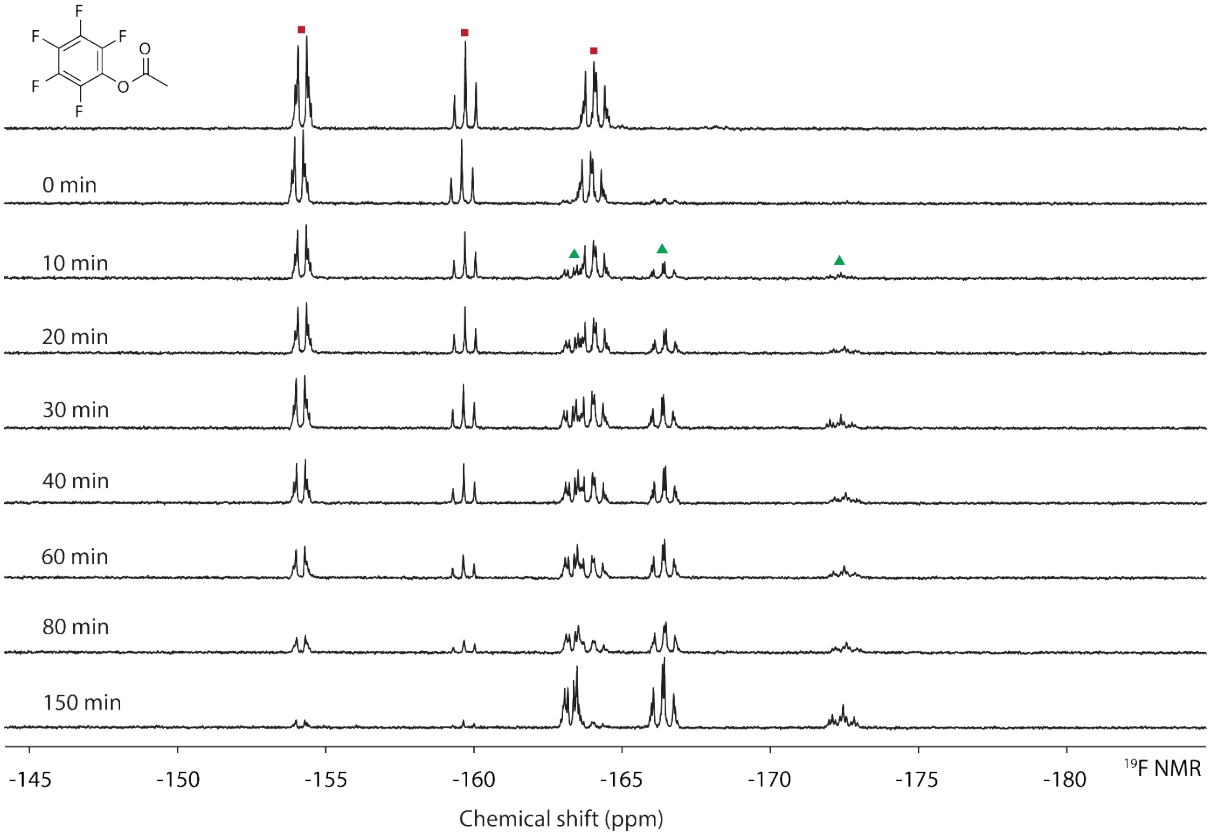

Figure S16. Time-dependent ^{19}F-NMR monitoring for transesterification reaction of **Sub-4** and methanol with cat. 10 mol% [Zn**L**]$_n$ (red: substate, blue: pentafluorophenol).

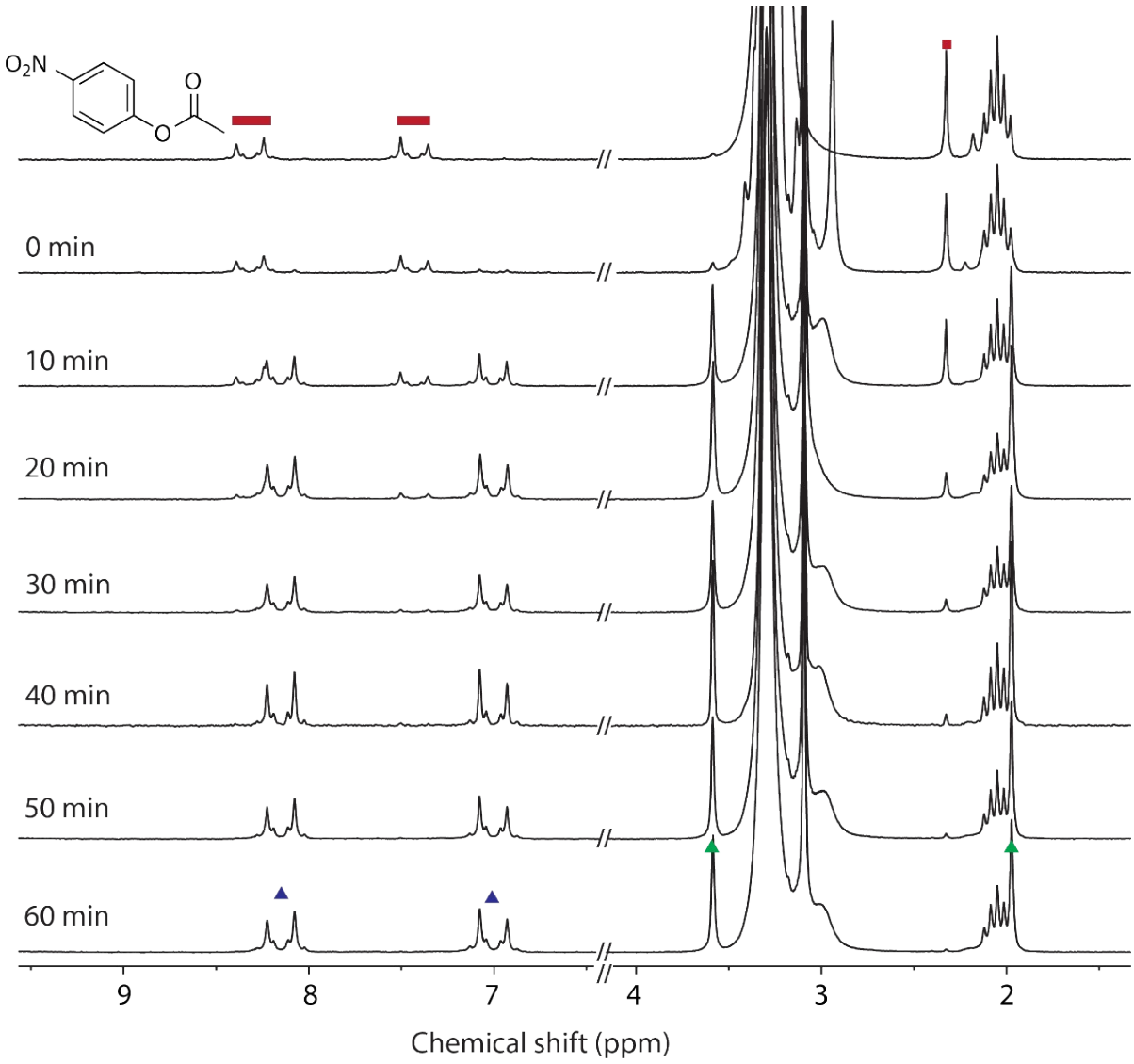

Figure S17. Time-dependent NMR monitoring for transesterification reaction of 4-nitrophenyl acetate (**Sub-5**, 500 μmol, 91 mg) and methanol with cat. 10 mol% (19.5 mg) [Zn**L**]$_n$ (red: substate, green: methyl acetate, blue: 4-nitrophenyl).

Sample	Reaction time	Starting / Product (Area)	Starting / Product (ratio)
Sub-1	50 min	5.06 / 0.37	93 / 7
	100 min	3.51 / 0.80	81 / 19
Sub-2	50 min	0/2.99	0 / 100
	100 min	0/3.51	0 / 100
Sub-3	50 min	0.45/2.18	17 / 83
	100 min	0/1.57	0 / 100
Sub-4	50 min	3.19/0.316	91 / 9
	100 min	1.34/0.85	61 / 39

Figure S18. Substrate-dependent catalytic yield that measured by GC-MS after the reaction with methanol and 10 mol% $[Zn\mathbf{L}]_n$ at 50 min and 100 min.

4.2 Recyclability experiment

To test the recyclability of [Zn**L**]$_n$ catalyst, the transesterification reaction (10 mol% [Zn**L**]$_n$) was conducted on **Sub-2** with methanol up to 5 cycles with the same conditions previously reported. After each cycle, the catalyst was recovered by filtration, washed with methanol and the checked by PXRD. From the second cycle, the reaction required longer time to reach full conversion of the substrate, as monitored by NMR spectroscopy. We performed the reaction until full conversion, to avoid possible contaminations from the substrate to the subsequent cycles.

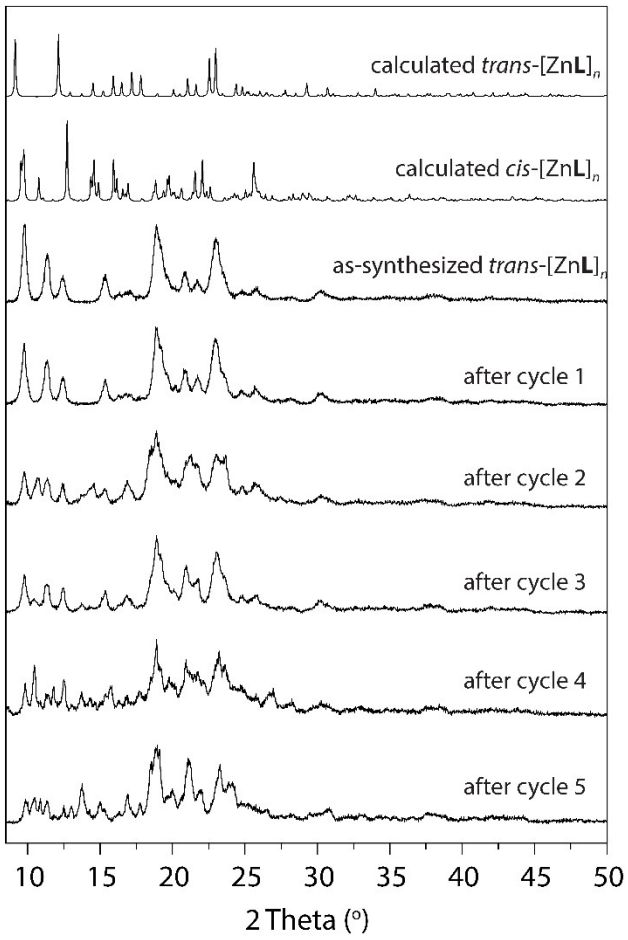

Figure S19. Calculated powder XRD patterns of *trans*-[Zn**L**]$_n$ and *cis*-[Zn**L**]$_n$, as-synthesized [Zn**L**]$_n$, and after up to 5 cycles of catalytic reactions.

Cycle	Yield (1h) (%)	Yield (1.5h) (%)	Yield (2.5h) (%)	Yield (3.5h) (%)	$[ZnL]_n$ recovery after catalysis (%)
1	94.2	100			97
2	84.0	92.3	100		99
3	77.9	85.8	100		91
4	--	--	67	100	90
5	--	--	--	100	99

Table S3. Recyclability of $[ZnL]_n$: yield for transesterification reaction of *p*-tolyl acetate (**Sub-2**) after 5 catalytic cycles and catalyst recovery yield after each cycle.

4.3 Experiment for switching effect in Catalysis for Transesterification

The on/off switching of the catalytic properties is carried out by removing or adding Cl^- to the system. To remove the anion, employing a silver salt in the form of $AgClO_4$, lead to precipitation of insoluble AgCl and consequent anion exchange of Cl^- with ClO_4^-, the latter being the same anion employed in the synthesis of the coordination polymer. On the other hand, addition of NH_4Cl leads to the reverse anion exchange, where Cl^- coordinate to Zn(II). The choice of NH_4^+ as a cation relies on the fact that the remaining NH_4^+ and ClO_4^- does not interfere with the studied reactions.

4.3.1 Turning on catalytic effects using silver(I) perchlorate

In a 2 mL vial, a methanol solution containing dispersed crystalline solid of $[Zn_2Cl_4\mathbf{L}]$ (16.7 mg, 25 μmol) was prepared. A methanol solution of 4 equiv. of $AgClO_4$ (20.7 mg, 100 μmol) was slowly added to the reaction vial. The mixture was vigorously stirred at 50 ℃ for 1 h, resulting in grey-colored precipitate. Subsequently, **Sub-2** in methanol was added into the reaction solution (the mole ratio of substrate and catalyst is 20:1) and stirred at 50 ℃. After 60 min and 90 min, ^{1}H NMR spectra were obtained and integrated for reaction yield. Then the precipitate was filtered and the residue was prepared to obtain the Powder XRD pattern and used as a catalyst for transesterification.

4.3.2. Turning off catalytic effects by adding chloride

In a 2 mL vial, a methanol solution containing dispersed crystalline solid of $[Zn\mathbf{L}]_n$ (19.5 mg, 25 μmol) was prepared. A methanol solution of 2 equiv. of NH_4Cl (2.7 mg, 50 μmol) was dropwisely added to the reaction vial. The mixture was vigorously stirred at 50 ℃ for 1 h. Subsequently, **Sub-2** (75 mg, 500 μmol) in methanol was added into the reaction solution (the mole ratio of substrate and catalyst is 20:1) and stirred at 50 ℃. After 60 min and 90 min, ^{1}H NMR spectra were obtained and integrated for reaction yield. After filteration and dying, the residue was prepared to obtain the Powder XRD pattern and used as a catalyst for transesterification.

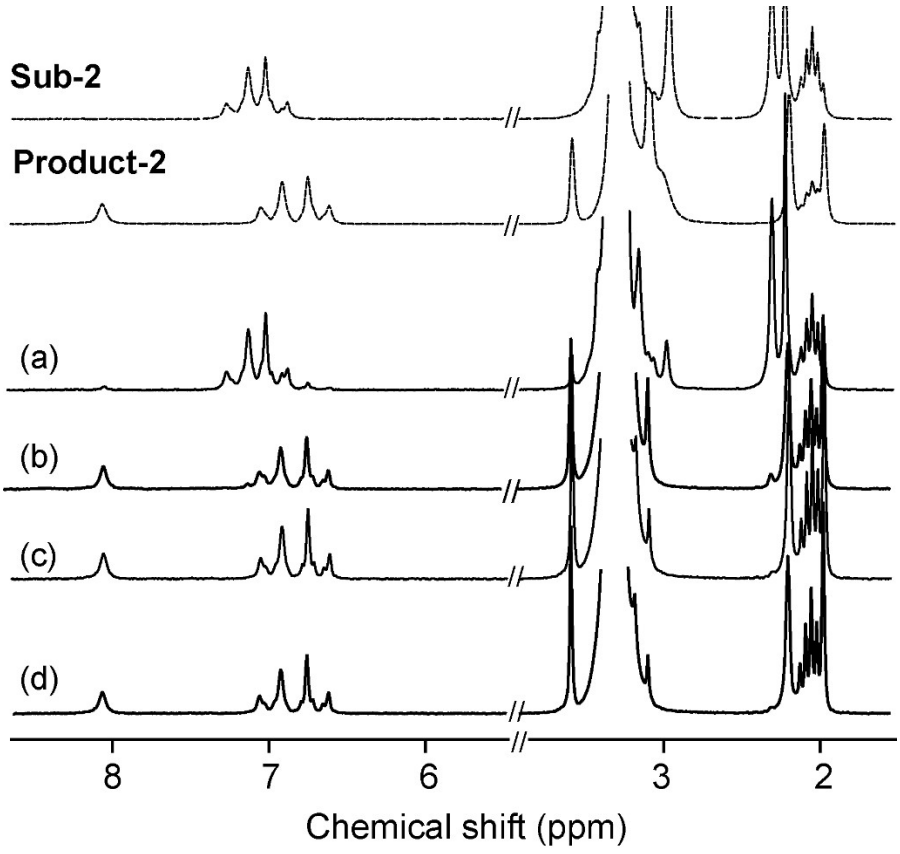

Figure S20. ^{1}H NMR data showing the catalytic switching effect controlled by anion exchange, the catalytic yields after 1 h reaction of **Sub-2** and [Zn_2Cl_4**L**] (a). Subsequently, stochiometric equivalent of $AgClO_4$ was added into reaction solution of (a) and reacted for 1 h (b) and 1.5 h (c), respectively. A catalytic yield at 1.5 hr reaction from the mixture of [Zn_2Cl_4**L**], $AgClO_4$, and **Sub-2** (d).

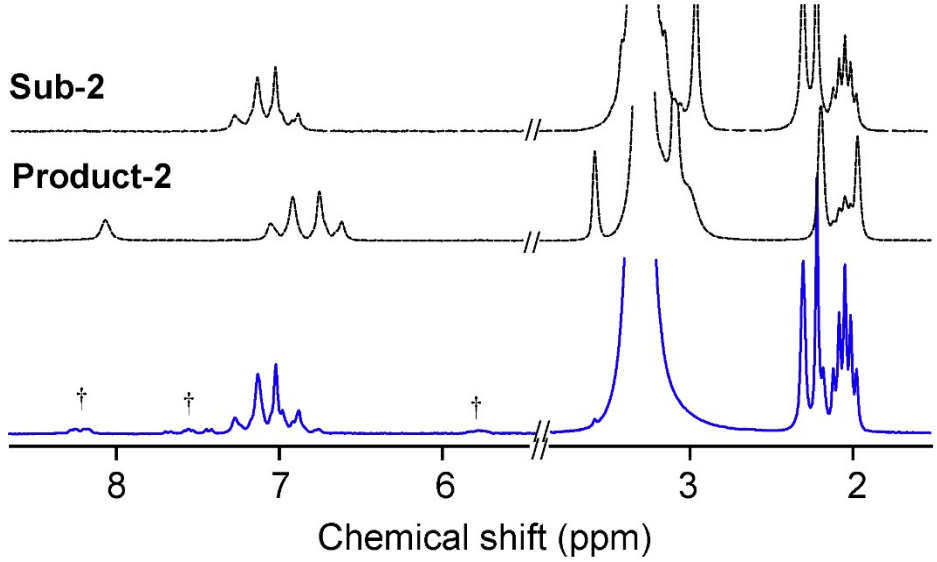

Figure S21. In-situ catalytic reaction of **Sub-2** monitored by ^{1}H NMR spectra after anion exchange from [Zn**L**]$_n$ using NH_4Cl. Reaction condition: **Sub-2** (75 mg, 25 μmol); [Zn**L**]$_n$ (19.5 mg, 500 μmol), NH_4Cl (2.7 mg, 50 μmol) for 1.5 h reaction in 500 μL methanol (blue), dagger represents free **L**.

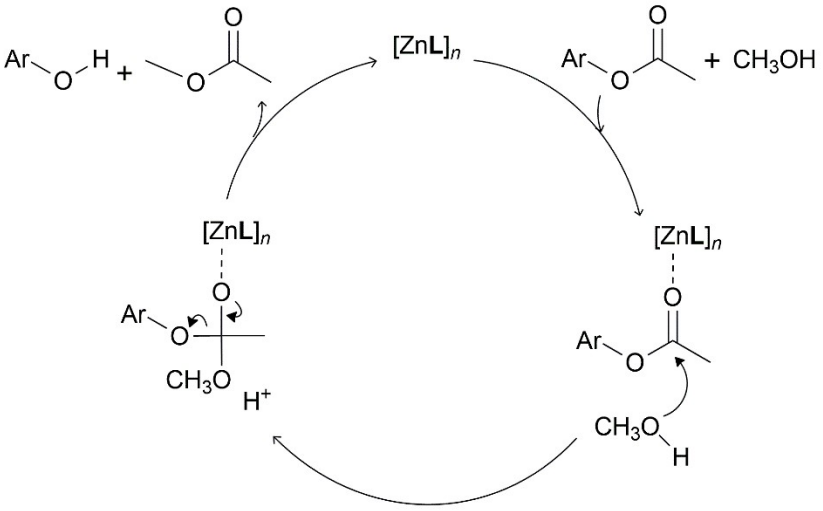

Figure S22. Proposed mechanism for transesterification using [Zn**L**]$_n$.

5. Reference

1 G. M. Sheldrick, SHELXT – Integrated space-group and crystal-structure determination, *Acta Crystallogr. Sect. A Found. Adv.*, 2015, **71**, 3–8.

2 G. M. Sheldrick, Crystal structure refinement with SHELXL, *Acta Crystallogr. Sect. C Struct. Chem.*, 2015, **71**, 3–8.

3 C. B. Hübschle, G. M. Sheldrick and B. Dittrich, ShelXle : a Qt graphical user interface for SHELXL, *J. Appl. Crystallogr.*, 2011, **44**, 1281–1284.